Int. J. Nonlinear Anal. Appl. 14 (2023) 1, 2701–2715
ISSN: 2008-6822 (electronic)
http://dx.doi.org/10.22075/ijnaa.2023.29382.4144

# Improved image segmentation method based on optimized higher-order polynomial

Anmar Jameel Naji, Shehab A. Ibrahem*, Shahla U. Umar

*Department of Computer Science, College of Computer Science and Information Technology, University of Kirkuk, Kirkuk, Iraq*

*(Communicated by Ehsan Kozegar)*

**Abstract**

Image segmentation is an essential task in images analyzing images. At the pixel level, the images characterize as: 1) an object from its background, or 2) the rest of the objects from each other. Therefore, image segmentation refers to applying a vast diffusion over several domains. This article proposes an improved image segmentation method. To get the segmented image, we determine the multi-thresholds by minimizing a higher-order polynomial curve fitting for an image and choosing the best threshold. The method can be utilized on grey images. The findings demonstrate that our method is effective and robust in image segmentation.

Keywords: Image segmentation, Polynomial function, Optimization
2020 MSC: 90C23

## 1 Introduction

Recent decades have seen rapidly growing research in many areas of computer science, including computer vision. Computer vision uses image features taken from cameras, scanners, and others. While the images cannot be understood directly, image segmentation isolates the object from the background. Furthermore, to perform segmentation, there is no procedure or a unified way. Therefore, image segmentation aims to expand the possibility of interpreting or analyzing existing information for human observers. To achieve this goal, image segmentation distributes pixels based on the difference in color intensity for classes and converts them into a digital image for processing.

### 1.1 Background

Image elements are usually observed as pixels, which are a group assortment of values used to represent a two-dimensional image in digital form. Any pixel's intensity is represented by a numerical value in a passing monochrome or grayscale image (see Figure 1) [33]. Image segmentation is one of the most significant issues in image processing and analysis. It involves segmenting the image into some sections that satisfy a particular uniformity requirement. The primary goal of segmentation is to make the analysis and declaration of various topics more easily represented and stated. For this aim, important regions of equal brightness can be extracted from an image [17, 20, 41]. Image segmentation is the basis for specifying the limits of object positions [1, 31, 37].

*Corresponding author
*Email addresses:* anmarjameelnajiabbood@gmail.com (Anmar Jameel Naji), mullaiq@uokirkuk.edu.iq (Shehab A. Ibrahem), Shahla_umar@uokirkuk.edu.iq (Shahla U. Umar)

*Received:* October 2022 *Accepted:* January 2023

In the literature, various studies proposed different segmentation methods, including threshold-based (T) segmentation algorithms. It is simple and easy to implement. To select thresholds, the graphing (T) segmentation algorithms employ a gray level by separating classes. This process is called a two-level threshold in case of separating an object from the background. To create two categories, the value of one threshold is used. Furthermore, the literature revealed that the two-level threshold is easier to implement than the multi-level Threshold (MT). Thus (MT) is more complex and provides more categories [30].

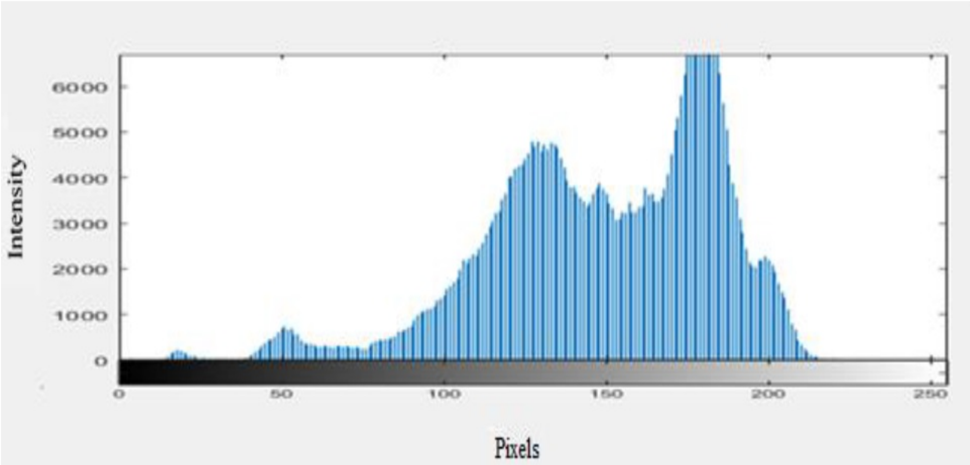


Figure 1: An image histogram

### 1.2 Paper Contributions

This article implements a higher-order polynomial curve fitting function for image segments based on image pixels and their intensity. In the literature, we can find mathematical expressions of different degrees of polynomial functions. We selected implementing a higher-order polynomial equation to an image to achieve better segmentation. In the performance analysis, we also used several criteria to measure image quality. Based on the segmented images' findings, our proposal is expected to offer noteworthy results over existing methods since it can calculate the minimum within multi-threshold objective methods [2].

### 1.3 Paper Organization

The rest of this article is structured as follows. Section 2 introduces some proposed studies in image segmentation. Section 3 presents some required definitions and assumptions related to our work. Section 4 presents our proposed method. Our experiment results are reported in Section 5. We conclude the paper with some future directions in Section 6.

## 2 Literature Review

As mentioned earlier, image segmentation refers to the process of dividing the image into multiple parts. It aims to make the image depiction within an easy concept to express and study more efficiently. It is essential to interpret and constructively analyze medical images [22]. Fragmentation is an advanced technology used to segment digital images based on the pixel's value to parts or multiple segments. Furthermore, fragmentation is crucial to discover images' system [33, 38]. We summarize here some critical techniques used to obtain the best image segmentation.

1. **Flood Fill**: In 2016, the authors Ashwaq T. Hashim, Duaa A. Noori in [14] proposed a technique based on a seed-fill algorithm or flood-fill algorithm to assign regions related to a specific node within a multi-dimensional array. The algorithm can be used for region-filling when all region pixels have the same features [11].
2. **Firework Algorithm**: In 2017, P.R. Misra and T. Si, in [21], suggested the fireworks algorithm to optimize micro-functions. The idea of the algorithm is based on the idea of exploding fireworks. It is represented by identifying four basic steps: Explosion process, base mapping, mutation process and selection strategy. By selecting a portion of the random points confined to a section of the distance scales, a large solution space is found. The study [21] can be employed as a tool for image segmentation [11].

3. **Fuzzy Tools**: In 2018, Venketkumar Hariraj introduced a new technique for describing human language rules [13]. Fuzzy logic and fuzzy set theory are the most prominent power tools in the form of fuzzy if-then rules. Similarly, in 2003, Mike Nachtegael et al. in [23] presented an image segmentation method based on four main algorithms: 1) Fuzzy C-mean clustering, 2) Fuzzy thresholding, 3) Fuzzy integral-based decision, and 4) Fuzzy rule-based inferencing scheme [11].
4. **Attention U-Net**: In 2018, Oktay et al. [25] used a deep learning (DL) technique to improve the diagnosis of COVID-19 accuracy classification. According to the literature, DL techniques can be used in medical images to capture fine structures. The feature helps segment lesions and lung nodules in COVID-19 patients [34].
5. **U-Net**: C. Zheng et al. proposed it in 2020 to segment lung regions and lesions in COVID-19 diagnosis applications [6, 15, 26, 40]. It is a fully convolutional network [28], a U-shaped architecture with symmetrical encoding and decoding signal paths. Short links connect the seams of the same plane in two paths. This allows the network to learn better visual semantics. The detailed contexts of U-Net are more suitable for medical image segmentation. To achieve excellent COVID-19 classification, many U-Net technique types were developed [34].
6. **Bayesian Convolutional Neural Network**: It was proposed by Ghoshal et al. in 2020 [9] to estimate the diagnosis uncertainty in COVID-19 prediction. The authors used 70 chest x-ray images of COVID-19 patients and non-COVID-19 images from (Pneumonia) from Kaggle [7]. The accuracy of detection reached 92.9% showing an improved detection of COVID-19 infections. Furthermore, conducted network saliency maps to illustrate the locations focused. Consequently, to facilitate a more informed decision-making process adding to improve the understanding of deep learning results [34].
7. **The Lattice Boltzmann method (LBM)**: S. Suman Rajest et al., in 2020, proposed a technique that utilized the parallel grid method to solve the level adjustment equation (LSE). LBM is faster than the pixel field because it decomposes in the graph space [8, 18, 29, 35]. Furthermore, LBM in breast MRI is more efficient and faster [12, 24, 32, 36]. Moreover, the LBM is a pixel-based algorithm that deals with particles. Here, the pixels are replicas of particles, and the algorithm can be tuned using various lattice points. Besides, LBM has the advantage of being able to be redefined in the microscopic domain. However, LBM suffers from difficulty in getting a regular structure in a medical image [27].

## 3 Preliminaries

The following assumptions and definitions are described for the reader's convenience.

### 3.1 Image histogram

An image histogram is the simplest technique for segmenting images is histogram thresholding, which is rapid and efficient in computation. A threshold based on brightness constants is employed to differentiate between background and objects. Band thresholding, local thresholding, multi-thresholding, and semi-thresholding represent a few modifications of this technique. While global thresholds are single thresholds implemented to the whole image, the local thresholds are single thresholds that may affect specific image portions [16]. The histogram shows the distribution of pixels and their chromatic intensity. Therefore, our study depends on the multi-thresholds by passing a high-order polynomial between the pixel and its intensity.

### 3.2 Polynomial curve fitting

Assume we have some measured data where $(x_i)$ and $(y_i)$ define a given problem. The Higher-degree polynomial is considered the most common method of representing and connecting the data and obtaining a smoothing function:

$$p(x) = p_n x^n + p_{2(n-1)} x^{n-1} + ... + p_1 x + p_0 \tag{3.1}$$

where $(p_0, p_1, ..., p_n)$ are the coefficients of the $p(x)$, and they can be solved using the following linear equations system.

$$\left\{ \begin{array}{llll} k & \sum_{i=1}^{k} X_i & \dots & \sum_{i=1}^{k} X_i^n \\ \sum_{i=1}^{k} X_i & \sum_{i=1}^{k} X_i^2 & \dots & \sum_{i=1}^{k} X_i^{n+1} \\ \vdots & \vdots & \vdots & \vdots \\ \sum_{i=1}^{k} X_i^n & \sum_{i=1}^{k} X_i^{n+1} & \dots & \sum_{i=1}^{k} X_i^{2n} \end{array} \right\} \left\{ \begin{array}{l} p_0 \\ p_1 \\ \vdots \\ p_n \end{array} \right\} = \left\{ \begin{array}{l} \sum_{i=1}^{k} Y_i \\ \sum_{i=1}^{k} X_i Y_i \\ \vdots \\ \sum_{i=1}^{k} X_i^n Y_i \end{array} \right\} \tag{3.2}$$

where $k$ refers to the number of points and $n$ denotes the degree of the polynomial function.

### 3.3 Measures of image quality

Here, we listed some approaches for evaluating image quality by comparing distorted image graphs to the original (distortion-free shots). Table 1 lists the most widely utilized measurements to assess the quality of an image [5, 19].

Table 1: Image characteristics parameters.

| Parameter | Acronym | Formulas Pattern |
|---|---|---|
| Mean Squared Error | MSE | $MSE = \frac{\sum_{i=1}^{M1}\sum_{i=1}^{M2}[f(i,j)-f'(i,j)]^2}{M1*M2}$ |
| Root Mean Square Error | RMSE | $RMSE = \sqrt{\frac{1}{n}\sum_{i=0}^{n}(y_i - y_i^n)^2}$ |
| Peak Signal-to-Noise Ratio | PSNR | $PSNR = 10\log\frac{(2^n-1)^2}{MSE} = 10\log\frac{255^2}{MSE}$ |
| Signal-to-Noise Ratio | SNR | $SNR = 10\log_{10}\left(\frac{\lambda^2}{\sigma^2}\right) = 10\log_{10}P^{-1}(N, 1-P_f)$ |

## 4 The proposed Method

This section presents a new method for finding the threshold based on the intensity chromaticity. The methodology of our work is as follows.

In the beginning, we pass the curve of higher order polynomial function $p_n(x)$ between pixels $x_i$ and their intensity $(y_i)$. It is possible to use a polynomial of different degrees. According to the image that becomes segmented, the higher degree of the polynomial will be. Consequently, we can get a better function to describe the image data. Next, we find a set of multi-threshold by minimizing the polynomial function $p_n(x)$ and get the best threshold depending on the best PSNR. We used a polynomial $p_{12}(x)$ of degree (12) and upwards to curve fitting the pixels $(x_i)$ and their intensity $(y_i)$.

$$p_{12}(x) = p_{12}x^{12} + p_{11}x^{11} + ... + p_1x + p_0 \tag{4.1}$$

Now, we need to solve (4.1) to obtain the suitable polynomial function, coefficients $(p_0, p_1, ..., p_{12})$ must be calculated. We can get one of any local search methods to determine the local minimizers of the function $p_{12}(x)$ (represents the image's multi-thresholds). Here, we use Newton Raphson's method as follows:

**Step 1**: Choose an initial point $x_0 \in x_i,\ \in > 0$.

**Step 2**: Set m=0.

**Step 3**: Calculate $x_1 = x_0 - \frac{p_{12}(x_0)}{p'_{12}(x_0)}$.

**Step 4**: Set $m = m + 1$ and continue in the iterative processes, $x_2 = x_1 - \frac{p_{12}(x_1)}{p'_{12}(x_1)}$ until we get $|x_{n+1} - x_n| <\in$ then consider $x_{n+1}$ is one of the image's thresholds.

Finally, Figure 2 illustrates the flowchart of performing the proposed method steps.

## 5 Experimental Results and Discussion

We applied our proposal to the following images to demonstrate our method. We show the appearance of several samples and the best threshold by using the higher order of polynomials.

### 5.1 Examples

**Example 1:**

As shown in Figure 3, we selected an onion. While, Figure 3(a) shows the original image, the Image Histogram and Image Curve fitting using the proposed method are illustrated in Figure 3(b and c). In Figure 3(c), the image analysis shows the distribution of pixels and the pixel intensity. The blue line represents the chromatic intensity, and the red line represents a polynomial curve of a high order from degree (30). For this example, Figure 4 shows the thresholds gained represent a group of samples to obtain the best segmentation. The best result can be observed among the other thresholds when the threshold equals (79). By contrast, the worst threshold reached (13) for the lack of fragmentation from the original image (Onion).

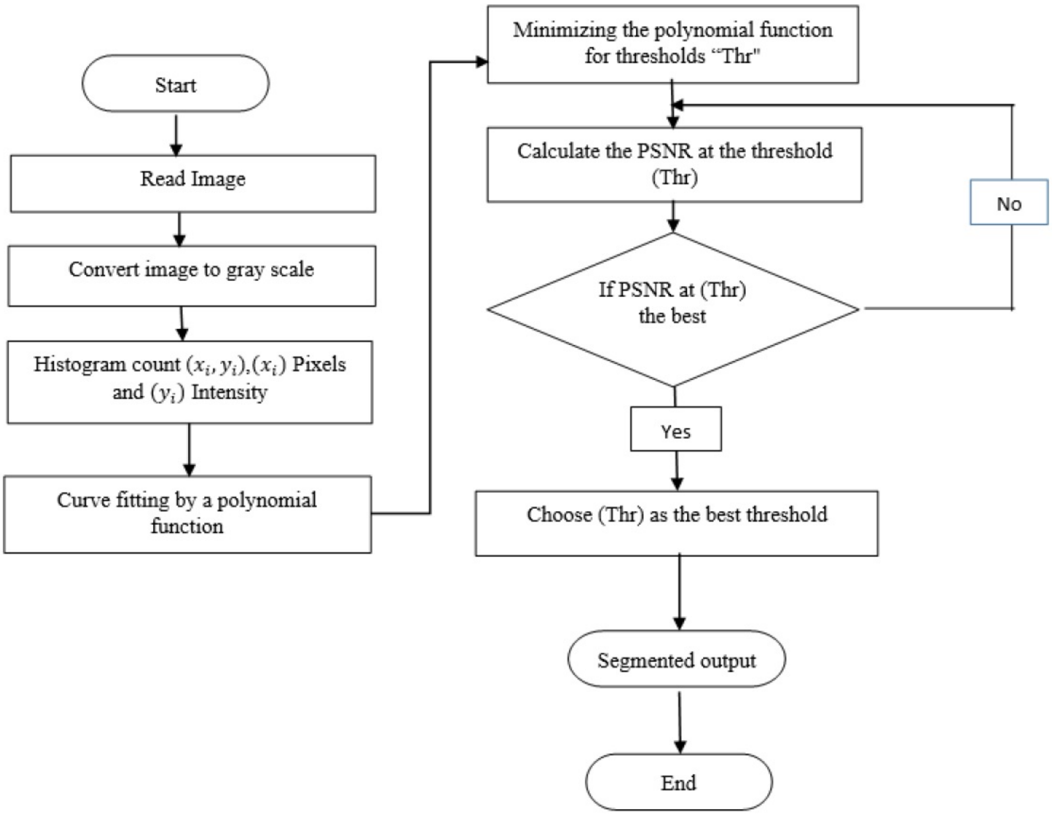


Figure 2: The flowchart of the proposed method.

(a)

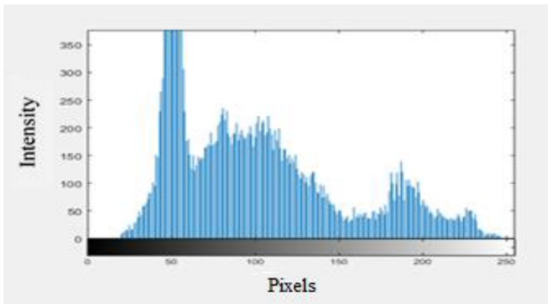


(b)

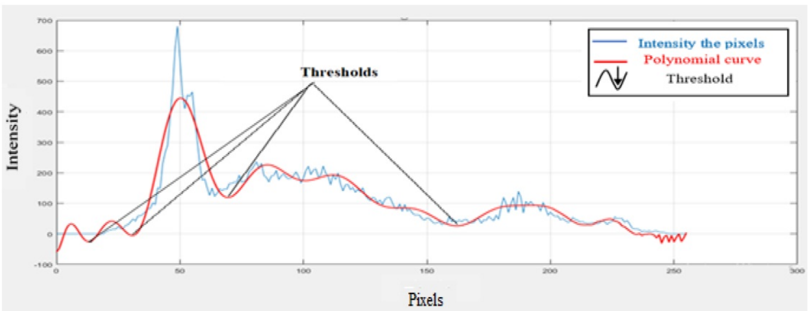


**(c)**

Figure 3: (a) Original Image1 (Onion), (b) Image Histogram using the proposed method, and (c) Image Curve fitting using the proposed method.

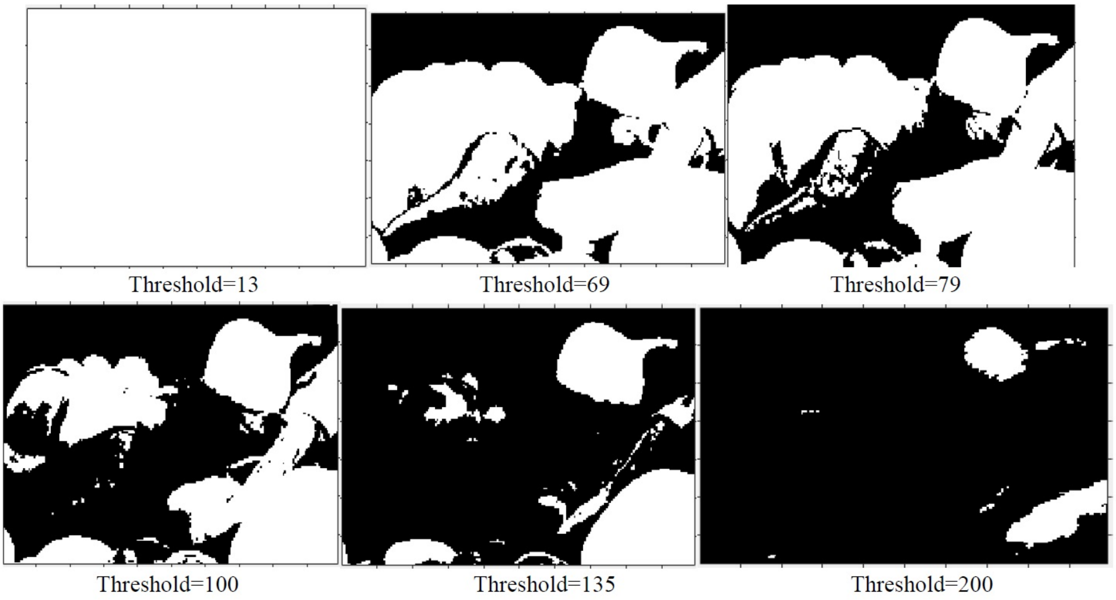


Figure 4: Thresholds of example 1.

**Example 2:**

In the second example, we used the (Lena) image. Similar to above, Figure 5(a) shows the original image, and the Image Histogram and Image Curve fitting using the proposed method are drawn in Figure 5(b and c). It is clear from Figure 5(c) there is a difference in pixel distribution and chromatic intensity. Additionally, the segmentation result varies according to the difference in the threshold obtained in our method through a higher-order polynomial (see Figure 6). The values of the thresholds revealed differences in image segmentation. Note that the segmentation does not appear clearly where the threshold is (180). Conversely, the best segmentation result appears when the threshold is (99).

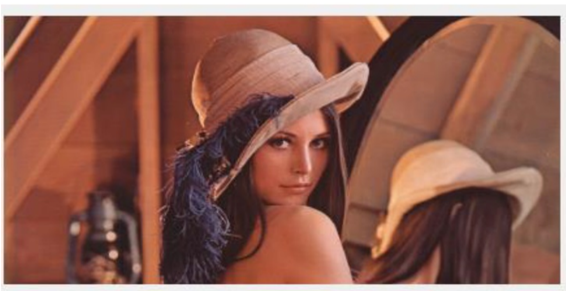

(a)

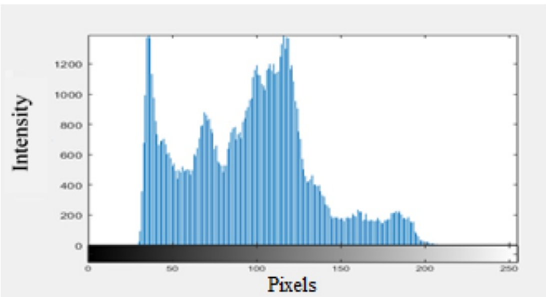


(b)

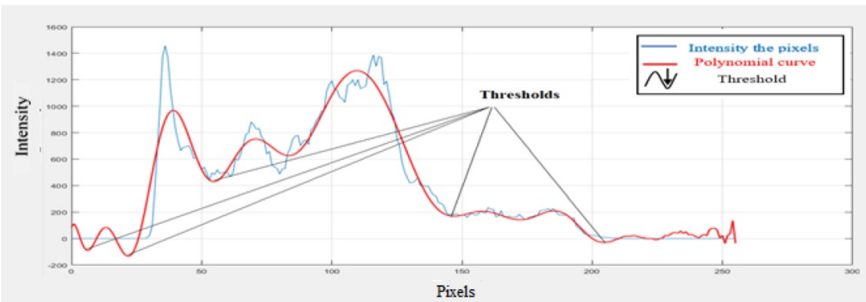


**(c)**

Figure 5: (a) Original of Image2 (Lena). (b) Image Histogram using the proposed method. (c) Image Curve fitting using the proposed method.

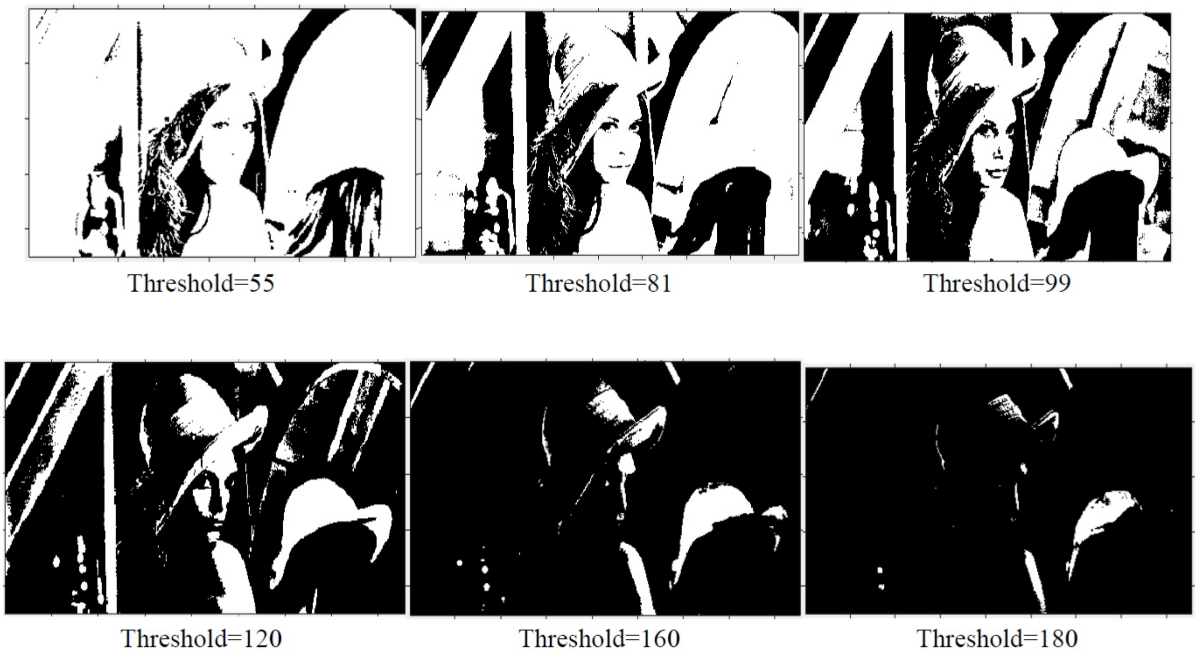


Figure 6: Thresholds of example 2.

**Example 3:**

In this example, we choose a cameraman image. Similar to previous examples, we draw in Figure 7(a) shows the original image, and the Image Histogram and Image Curve fitting using the proposed method are drawn in Figure 7(b and c). Figure 7(c) shows the distribution of pixels with their chromatic intensity by applying our method with polynomials of a higher degree order (30). Figure 8 show that the method produces various thresholds, each showing the image segmentation. Specifically, the result is not satisfactory when the threshold reaches (209). By contrast, the best result was achieved when the segmentation in threshold equals (122).

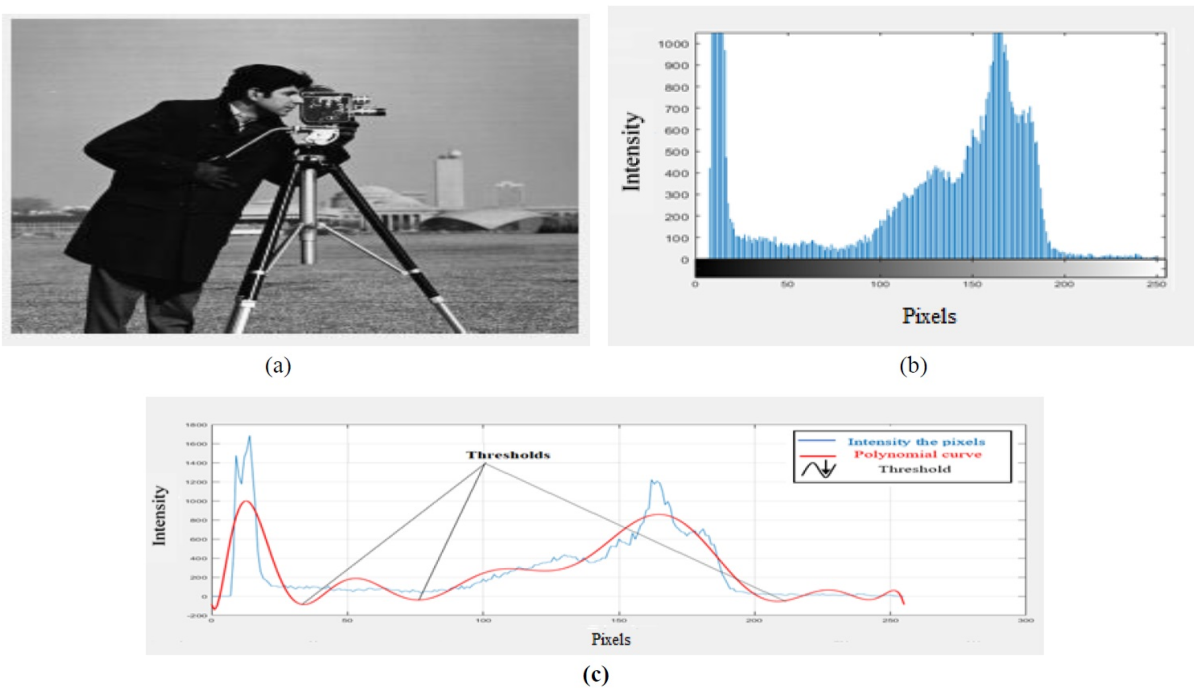


Figure 7: (a) Original Image3(Cameraman). (b) Image Histogram using the proposed method. (c) Image Curve fitting using the proposed method.

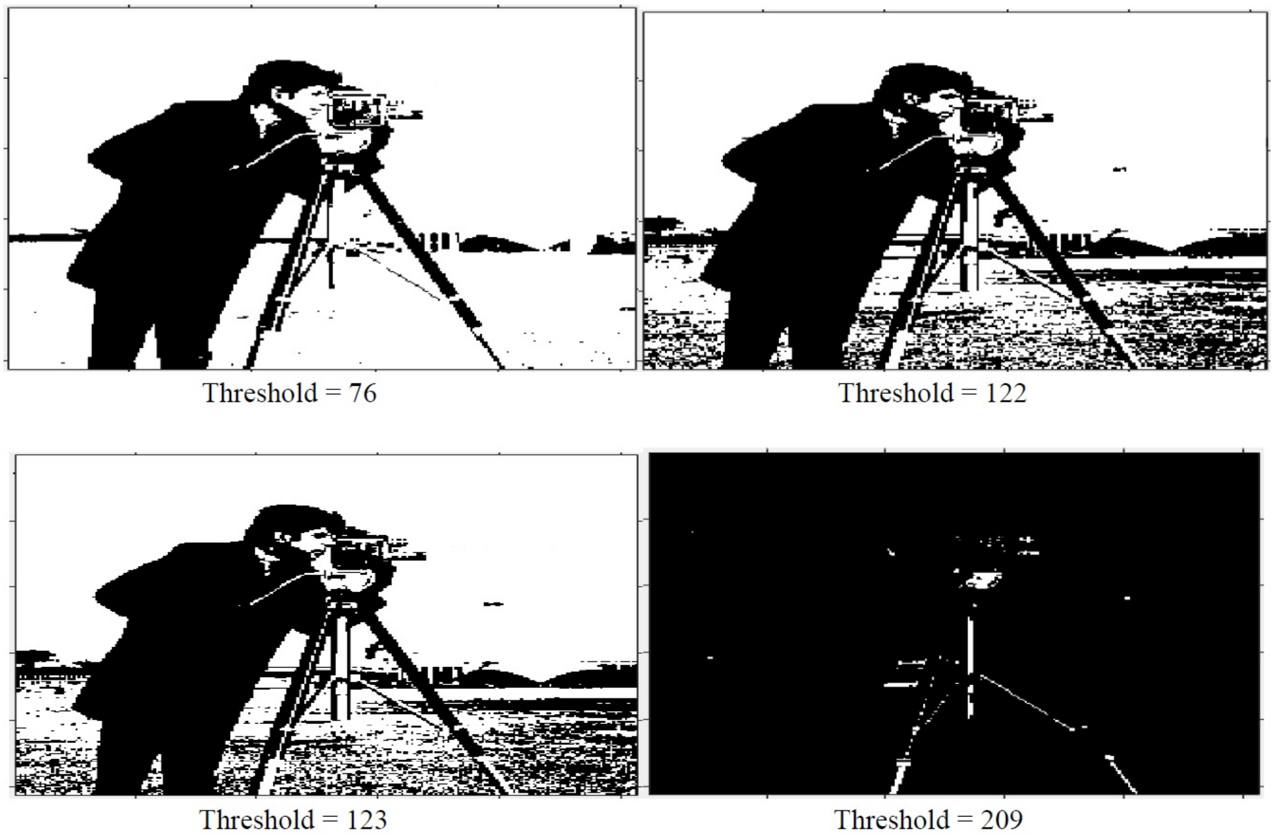


Figure 8: Thresholds of example 3.

Before delving into the next examples, we discuss here the process of fitting the curve consists of the following. Using polynomial functions, we start building a mathematical function that harmonizes with the nearest form of data points. We obtain matching values for the polynomial from new graphical points based on a discrete set of points. Interpolation is used with the values of a specific function (x) for specific points (we focus on multiple choice). The bounds (P) should be unique and match the data to generate the best curve.

For better information extraction and optimization, the correlation of coefficient values and residual values are crucial in the difference in the functional data set. The average values of the data set adjust the image component to the occurrence of overlap between the higher-order values of the polynomial. The segmentation technique employs the thresholding strategy by applying the threshold value (Thr) from the data set using the formula (5.1). Following the segmentation of data sets, close matching is once more checked for the nearest average data set values. Any input images may be further efficiently segmented using higher-order polynomial function datasets to create better-segmented results.

$$Thr = \frac{\sum_{k=1}^{m}\sum_{l=1}^{n} x(k,l)}{m * n} \tag{5.1}$$

where $x(k,l)$ refers to a data set, and the height and breadth of the data set image are denoted $m$ and $n$, respectively.

Higher-order polynomials are more suitable for preserving all data in residuals and curve-fitting figures with different orders of polynomials. For further processing and information extraction from the image, we carry out all the data information on the image according to the appropriate curve. The above images reveal several thresholds for image segmentation. The best threshold with optimal segmentation can be determined to smoothly separate the object from the background. It is based on passing the curve between the pixel density represented by $(x_i)$ and the number of its intensity represented by $(y_i)$. The segmentation output is clear through analyzing the different test images, with clarity of the action proposed method in the research. Figures 3(b), 5(b), and 7(b) show the proposed output of the segmented images generated by our method.

### 5.2 Tests

**Test 1 and 2:**

To demonstrate the superiority of our method, we implement it over the images (Figures 9 and 10) used in [4]. The segmentation shows satisfactory results in Figures 9 and 10.

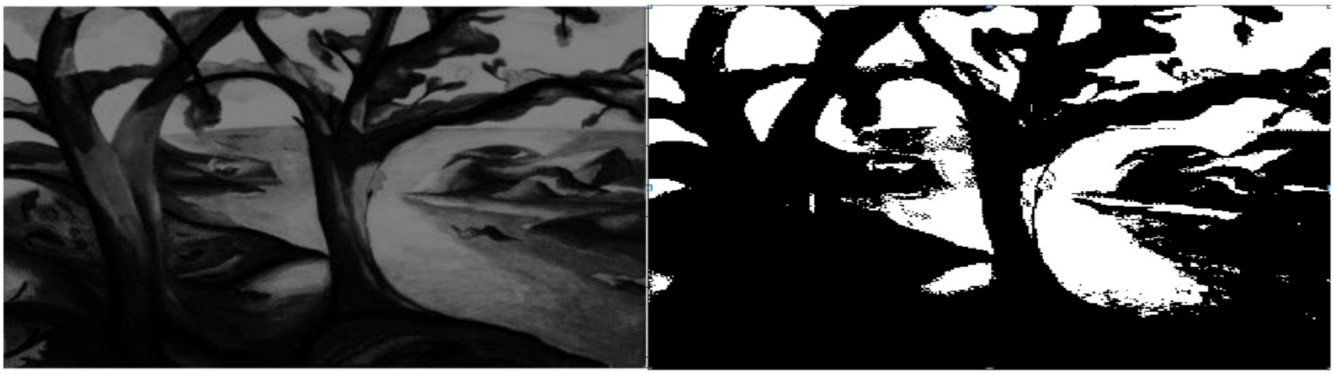

(a) (b)

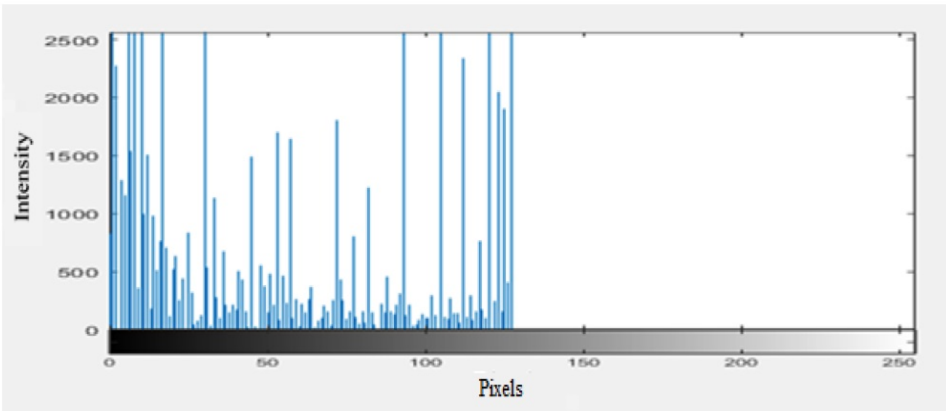


**(c )**

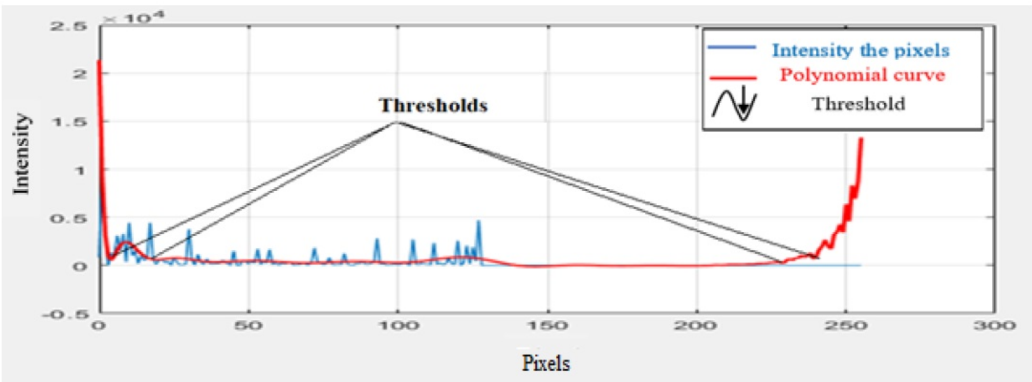


**(d)**

Figure 9: (a) Original Test 1(Tree). (b) Image Segmentation using the proposed method. (c) Image Histogram using the proposed method. (d) Image Curve fitting using the proposed method.

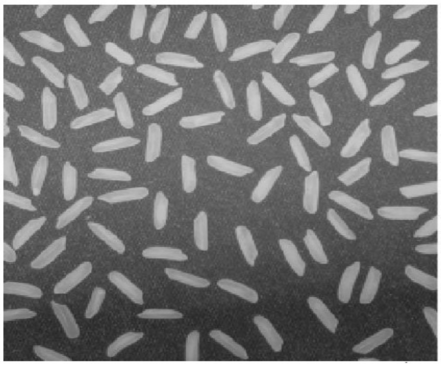
(a)

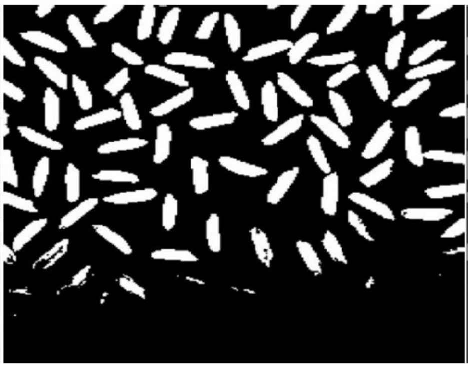
(b)


(c)

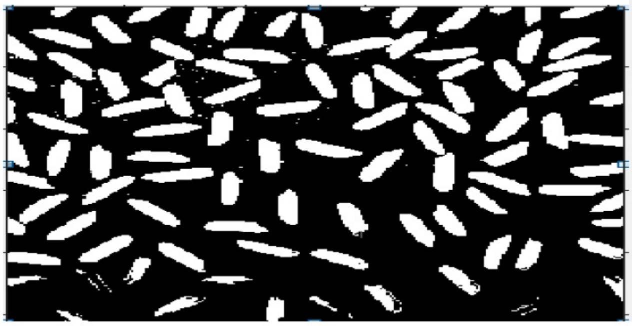
(d)

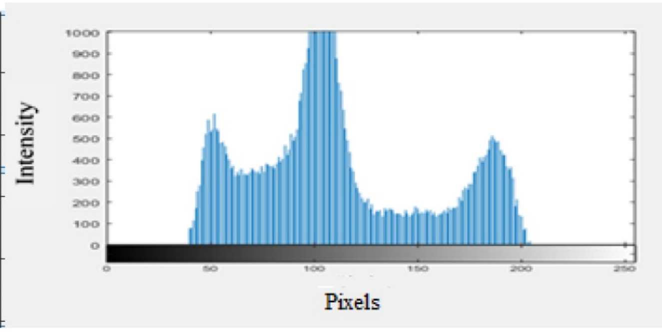

(e)

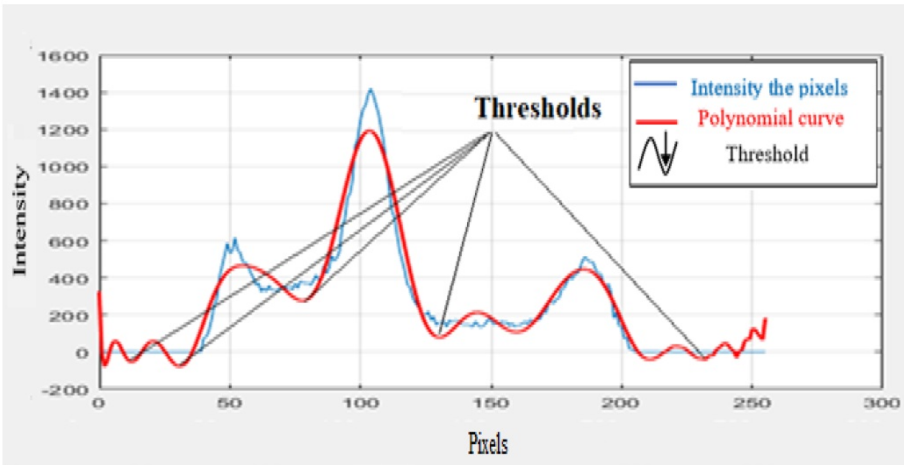

**(f)**

Figure 10: (a) Original Test 2 (Rice). (b) Ostu's Segmentation output. (c) Histogram-based segmentation output. (d) Image Segmentation using the proposed method. (e) Image Histogram using the proposed method. (f) Image Curve fitting using the proposed method.

**Tests 3 and 4:**

As shown in Figure 11(a), the proposed approach is more suitable for medical images. Using the proposed method, the results of the output images were entered and compared with other modern segmentation methods, namely the Otsu segmentation method and another graph-based method. Comparative results are presented in Figures 11 and 12. Medical imaging also produces a finely segmented result when using our proposed method. The segmented output images in Figures 10 through 12 (used in [4]) were produced utilizing the smoothing image segmentation technique of the curve fitting-based higher-order polynomial from degree (30) to pass the curve between distributed pixels and chromatic intensity. Inserted the polynomial curve diagram of our method and compared the obtained images with the images in the source [4].

Therefore, image quality evaluation is crucial for the image processing system. We reflected the quality measurement of the suggested method's results with other image segmentation techniques, such as the Histogram-based, Edge-Detection-Based, Ostu's, and Watershed approaches. For application noise, all test images have been picked. For application noise, all test images have been picked.

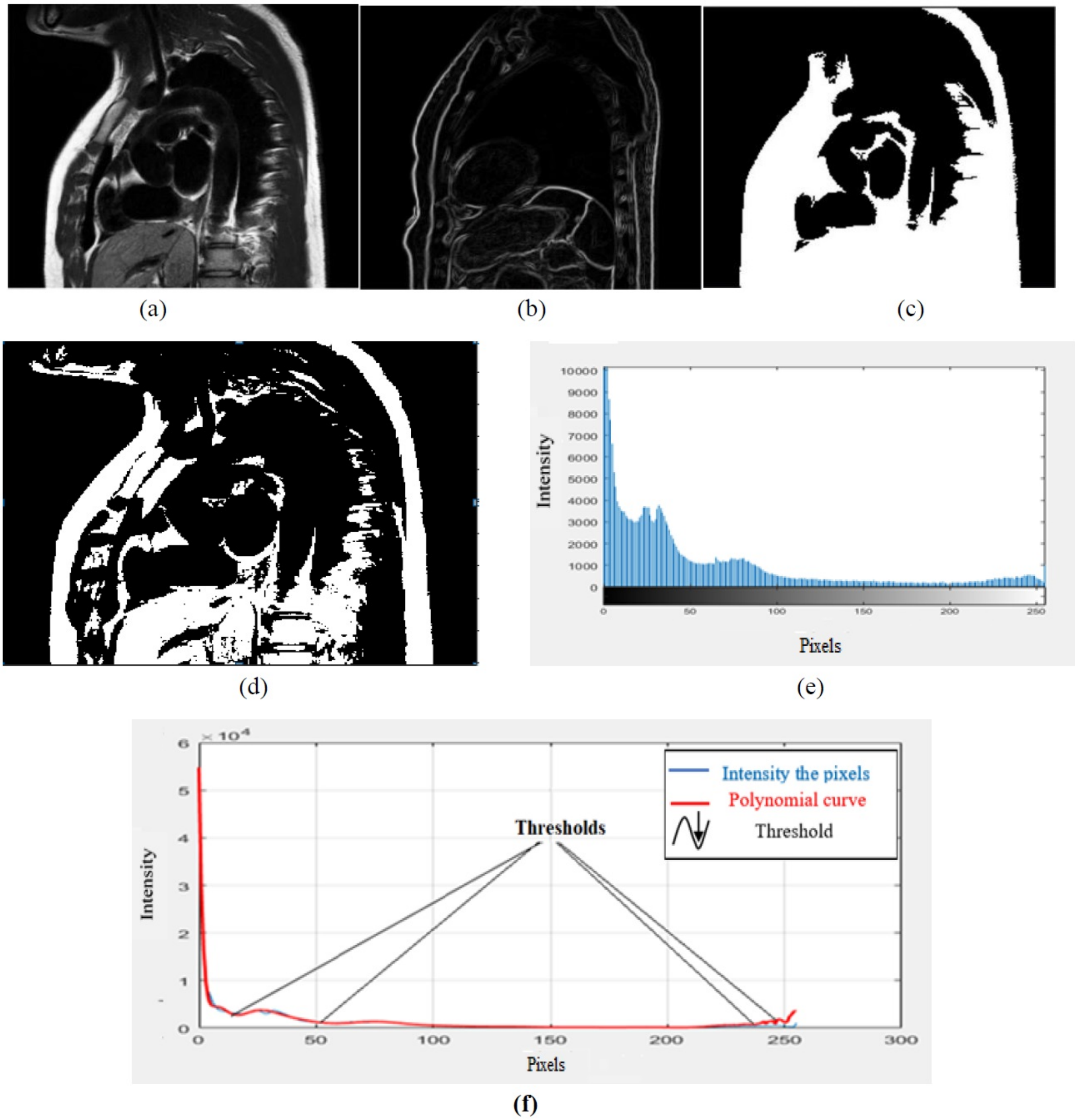


Figure 11: (a) Original Test 3. (b) Ostu's Segmentation output. (c) Histogram-based segmentation output. (d) Image Segmentation using the proposed method. (e) Image Histogram using the proposed method. (f) Image Curve fitting using the proposed method.

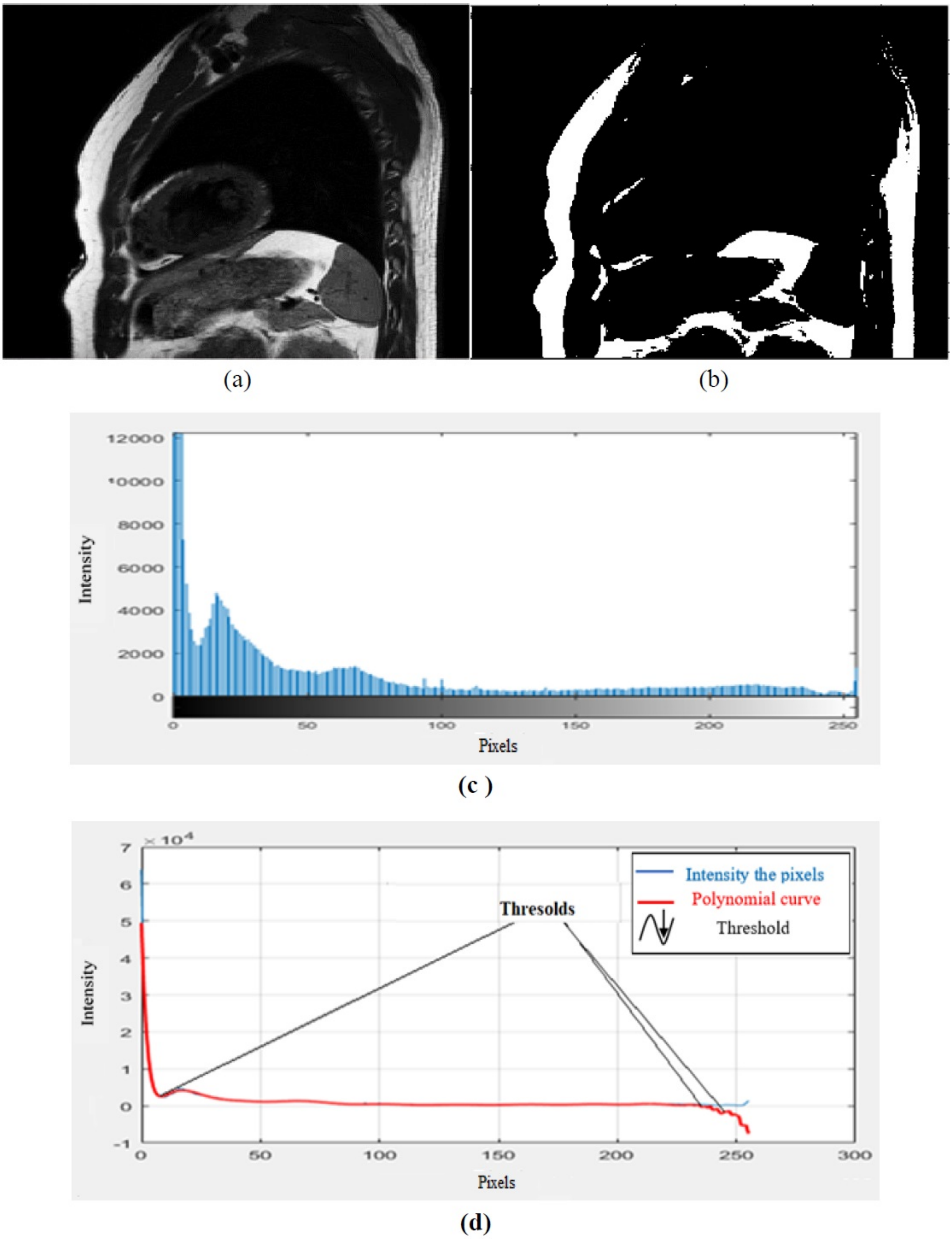


Figure 12: ((a) Original Test 4. (b) Image Segmentation using the proposed method. (c) Image Histogram using the proposed method. (d) Image Curve fitting using the proposed method.

Finally, the image quality assessment is necessary for the image processing system, to analyze the image quality metrics of the results image by the proposed method helps to clarify the conclusion of the examination of image quality metrics, and the parameters are calculated in connection with different noise models. Table 2 lists the calculated results of the Cameraman image with the different images taken for the test. Furthermore, as illustrated in Table 3, the proposed method achieved higher image quality to noise by getting higher PSNR values. When comparing the Universal Quality Index's with other current segmentation methods, such as watershed segmentation and Otsu's segmentation and other methods. Our proposed method's universal quality index values are higher than other segmentation methods, which points out the quality of results for images segmented by the submitted segmentation method. The submitted segmentation method supplies acceptable and exact results to segmentation images for bestead produced.

Table 2: Image quality evaluation

| No. | Experiment Inputs | MSE | RMSE | PSNR | SNR |
|---|---|---|---|---|---|
| 1 | Test 1 | 181.3730 | 13.4675 | +20.5168 | −7.0227 |
| 2 | Test 2 | 255 | 15.9687 | +17.3032 | −8.5024 |
| 3 | Cameraman | 237.8510 | 15.4224 | +17.9161 | −8.2000 |
| 4 | Mri | 88.1246 | 9.3875 | +29.4339 | −3.8879 |

Table 3: PSNR (db) comparison to the outcomes of other methodologies

| No. | Experiment Inputs | Histogram based Segmentation [10] | Otsu's Segmentation [39] | Edge Detection based Segmentation [10] | Watershed Segmentation [3] | Segmentation based Polynomial [4] | Our Proposed Technique |
|---|---|---|---|---|---|---|---|
| 1 | Test 1 | +13.79846 | +14.12834 | +15.21225 | +14.09275 | +15.33335 | +20.5168 |
| 2 | Test 2 | +13.98295 | +13.98655 | +14.91680 | +13.88677 | +15.29441 | +17.3032 |
| 3 | Cameraman | +15.00903 | +14.04588 | +14.89949 | +14.10470 | +15.11115 | +17.9161 |
| 4 | Mri | +14.92596 | +14.09313 | +15.21850 | +13.78341 | +15.58855 | +29.4339 |

## 6 Conclusion

In this paper, we proposed an improved image segmentation method. A comparative analysis of several segmentation method criteria has been presented. The proposed method combines the following: 1) The higher-order polynomial, which depends on passing a polynomial curve fitting between image pixels and the intensity of the pixels for the image; and 2) finding multi-thresholds for best image segmentation. The experiments on several examples demonstrated that our proposed method is effective and robust to image segmentation. Furthermore, various segmentation techniques have been compared versus the recommended curve fitting-based polynomial smoothing image segmentation methodology. Nevertheless, despite its simplicity and high efficiency, our method it's working to discover the object obviously and award more precision during the account of the quality index. Thus, the suggested method points out a hopeful future for evaluation research.

## References


[1] M. Abdulghafour, *Image segmentation using Fuzzy logic and genetic algorithms*, J. WSCG **11** (2003), no. 1.

[2] S. Akram and Q.U. Ann, *Newton raphson method*, Int. J. Sci. Eng. Res. **6** (2015), no. 7, 1748–1752.

[3] L.J. Belaid and W. Mourou, *Image segmentation: a watershed transformation algorithm*, Image Anal. Stereol. **28** (2009), 93–103.

[4] S. Biswas, D. Ghoshal and R. Hazra, *A new algorithm of image segmentation using curve fitting based higher order polynomial smoothing*, Optik **127** (2016), no. 20, 8916–8925.

[5] A.C. Brooks, X. Zhao and T.N. Pappas, *Structural similarity quality metrics in a coding context: exploring the space of realistic distortions*, IEEE Trans. Image Process. **17** (2008).

[6] Y. Cao, Z. Xu, J. Feng, C. Jin, X. Han, H. Wu and H. Shi, *Longitudinal assessment of COVID-19 using a deep learning–based quantitative CT pipeline: illustration of two cases*, Radiology: Cardioth. Imag. **2** (2020), e200082.

[7] J.P. Cohen, P. Morrison and L. Dao, *COVID-19 image data collection*, arXiv 2003.11597, (2020).

[8] D. Datta, S. Mishra and S.S. Rajest, *Quantification of tolerance limits of engineering system using uncertainty modeling for sustainable energy*, Int. J. Intell. Networks **1** (2020), 1–8.

[9] B. Ghoshal and A. Tucker, *Estimating uncertainty and interpretability in deep learning for coronavirus (COVID-19) detection*, arXiv:2003.10769, (2020).

[10] R.C. Gonzalez and P. Wintz, *Digital image processing*, 2nd ed. Addison-Wesley, Reading, MA, 1987.

[11] D.L.L. Gwet, M. Otesteanu, I.O. Libouga, L. Bitjoka and G.D. Popa, *A review on image segmentation techniques and performance measures*, Int. J. Comput. Inf. Eng. **12** (2018), no. 12, 1107–1117.

[12] A. Haldorai, A. Ramu and S. Murugan, *Social aware cognitive radio networks: effectiveness of social networks as a strategic tool for organizational business management*, Social network analytics for contemporary business organizations, IGI Global, 2018, pp. 18–202.

[13] V. Hariraj, W. Khairunizam, V. Vikneswaran, Z. Ibrahim, A.B. Shahriman, M.R. Zuradzman, T. Rajendran and R. Sathiyasheelan, *Fuzzy multi-layer SVM classification of breast cancer mammogram images*, Int. J. Mechanic. Eng. Technol. **9** (2018), no. 8, 1281–1299.

[14] A.T. Hashim and D.A. Noori, *An approach of noisy color iris segmentation based on hybrid image processing techniques*, Int. Conf. Cyberworlds (CW), IEEE, 2016, pp. 183–188.

[15] L. Huang, R. Han, T. Ai, P. Yu, H. Kang, Q. Tao and L. Xia, *Serial quantitative chest CT assessment of COVID-19: deep-learning approach*, Radiology: Cardioth. Imag. **2** (2020), e200075.

[16] M.S. Khadem, *MRI brain image segmentation using graph cuts*, Master's thesis, Chalmers University of Technology, Goteborg, Sweden, 2010.

[17] I.G. Khanykov, I.M. Tolstoj and D.K. Levonevskiy, *The classification of the image segmentation algorithms*, Int. J. Intell. Unmanned Syst. **8** (2020), no. 2, 115–127.

[18] E.L. Lidiya and S. Kannan, S.S. Rajest and S. Satyanarayana, *Correlative study and analysis for hidden patterns in text analytics unstructured data using supervised and unsupervised learning techniques*, Int. J. Cloud Comput. **9** (2020), no. 2/3.

[19] A. Liu, W. Lin and M. Narwaria, *Image quality assessment based on gradient similarity*, IEEE Trans. Image Process. **21** (2012), no. 4, 1500–1512.

[20] D.R. Martin, C.C. Fowlkes and J. Malik, *Learning to detect natural image boundaries using local brightness, color, and texture cues*, IEEE Trans. Pattern Anal. Machine Intel. **26** (2004), no. 5, 530–549.

[21] P.R. Misra and T. Si, *Image segmentation using clustering with fireworks algorithm*, 11th Int. Conf. Intel. Syst. Control (ISCO), IEEE, 2017, pp. 97–102.

[22] H.M. Moftah, A. TaherAzar, E.T. Al-Shammari, N.I. Ghali, A.E. Hassanien and M. Shoman, *Adaptive k-means clustering algorithm for MR breast image segmentation*, Neural Comput. Applic. **24** (2014), 1917–1928.

[23] M. Nachtegael, D. Van der Weken, D. Van De Ville and E.E. Kerre, *Fuzzy filters for image processing*, Springer-Verlag Berlin Heidelberg, 2003.

[24] A.J. Obaid, *Critical research on the novel progressive, JOKER an opportunistic routing protocol technology for enhancing the network performance for multimedia communications*, Res. Intell. Comput. Eng. Adv. Intell. Syst. Comput. **1254** (2021), 369–378.

[25] O. Oktay, J. Schlemper, L.L. Folgoc, M. Lee, M. Heinrich, K. Misawa, K. Mori, S. McDonagh, N.Y. Hammerla, B. Kainz and B. Glocker, *Attention U-Net: Learning where to look for the pancreas*, arXiv:1804.03999, (2018).

[26] X. Qi, Z. Jiang, Q. Yu, C. Shao, H. Zhang, H. Yue, B. Ma, Y. Wang, C. Liu, X. Meng and S. Huang, *Nachine learning-based CT radionics model for predicting hospital stay in patients with pneumonia associated with SARS-CoV-2 infection: A multicenter study*, MedRxiv, 2020.

[27] K.K.D. Ramesh, G.K. Kumar, K. Swapna, D. Datta and S.S. Rajest, *A review of medical image segmentation algorithms*, EAI Endorsed Trans. Pervasive Health Technol. **7** (2021), no. 27, e6.

[28] O. Ronneberger, P. Fischer and T. Brox, *U-Net: Convolutional networks for biomedical image segmentation*, Int. Conf. Medical Image Comput. Comput.-Assist. Intervent., 2015, pp. 234–241.

[29] L. Santoso, B. Singh, S.S. Rajest, R. Regin, K. Kadhim, *A genetic programming approach to binary classification problem*, EAI Endorsed Trans. Energy **8** (2021), no. 31, 1–8.

[30] P.D. Sathya and R. Kayalvizhi, *Optimal multilevel thresholding using bacterial foraging algorithm*, Expert. Syst. Appl. **38** (2011), no. 12, 15549–15564.

[31] N. Senthilkumaran and R. Rajesh, *Edge detection techniques for image segmentation—a survey*, Proc. Int. Conf. Manag. Next Gener. Software Appl. (MNGSA-08), 2008, pp. 749–760.

[32] S. Sharma and A.J. Obaid, *Mathematical modelling, analysis and design of fuzzy logic controller for the control of ventilation systems using MATLAB fuzzy logic toolbox*, J. Interdiscip. Math. **23** (2020), no. 4, 843–849.

[33] P. Sharma and J. Suji, *A review on image segmentation with its clustering techniques*, Int. J. Signal Process. Image Process. Pattern Recogn. **9** (2016), no. 5, 209–218.

[34] F. Shi, J. Wang, J. Shi, Z. Wu, Q. Wang, Z. Tang, K. He, Y. Shi and D. Shen, *Review of artificial intelligence techniques in imaginf data acquisition, segmentation, and diagnosis for COVID-19*, IEEE Rev. Biomed. Eng. **14** (2020), 4–15.

[35] B. Singh, P. Kavitha, R. Regin, K. Praghash, S. Sujatha and S.S. Rajest, *Optimized node clustering based on received signal strength with particle ordered-filter routing used in VANET*, Webology **17** (2020), no. 2, 262–277.

[36] M. Suganya and H. Anandakumar, *Handover based spectrum allocation in cognitive radio networks*, Int. Conf. Green Comput. Commun. Conserv. Energy (ICGCE), 2013.

[37] O.J. Tobias and R. Seara, *Image segmentation by histogram thresholding using fuzzy sets*, IEEE Trans. Image Process. **11** (2002), no. 12, 1457–1465.

[38] M. Xess and S.A. Agnes, *Survey on clustering based color image segmentation and novel approaches to FCM algorithm*, Int. J. Res. Eng. Technol. **2013** (2013), 346–349.

[39] J. Zhang and J. Hu, *Image segmentation based on 2D Otsu method with histogram analysis*, IEEE, Int. Conf. Comput. Sci. Software Eng. **6** (2008).

[40] C. Zheng, X. Deng, Q. Fu, Q. Zhou, J. Feng, H. Ma, W. Liu and X. Wang, *Deep learning-based detection for COVID-19 from chest CT using weak label*, MedRxiv, 2020.

[41] H. Zhu, F. Meng, J. Cai and S. Lu, *Beyond pixels: a comprehensive survey from bottom-up to semantic image segmentation and cosegmentation*, J. Visual Commun. Image Represent. **34** (2016), 12–27.